Molecular map of Chromosome 19 including three genes affecting bleeding time: *ep, ru,* and *bm*

E.P. O'Brien,[1] E.K. Novak,[1] S.A. Keller,[2] C. Poirier,[3] J.-L. Guénet,[3] R.T. Swank[1]

[1]Molecular and Cellular Biology Department, Roswell Park Cancer Institute, Carlton and Elm Streets, Buffalo, New York 14263, USA
[2]Department of Human Genetics, University of Michigan, Ann Arbor, Michigan 48109, USA
[3]Unité de Génétique des Mammiféres, Institut Pasteur de Paris, 75724 Paris Cedex 15, France

Abstract. The mouse ruby eye (*ru*) and pale ear (*ep*) pigment dilution genes cause platelet storage pool deficiency (SPD) and prolonged bleeding times. The brachymorphic (*bm*) gene, in addition to causing skeletal abnormalities, is also associated with prolonged bleeding times. All three hemorrhagic genes are found within 10 cM on Chromosome (Chr) 19. In this study, 15 microsatellite markers and five cDNAs, spanning 21 cM of Chr 19, were mapped in relation to the *bm, ep,* and *ru* genes in 457 progeny of an interspecific backcross utilizing the highly inbred strain PWK derived from the *Mus musculus musculus* species. Several markers were found to be closely linked to the three genes and should be useful as entry points in their eventual molecular identification.

Introduction

Platelet storage pool deficiency (SPD) is an autosomal recessive disorder characterized by a prolonged bleeding time and decreased contents of platelet dense and/or alpha granules (Witkop et al. 1989). After von Willebrand disease, it is the most common inherited hemorrhagic disease in humans, with an incidence as high as 1/2000 in some populations (Witkop et al. 1989; Nieuwenhuis et al. 1987; Israels et al. 1990). It occurs in patients with the inherited Hermansky-Pudlak syndrome (HPS; Witkop et al. 1989; Depinho and Kaplan 1985) and the fatal Chediak-Higashi syndrome (CHS) (Witkop et al. 1989; Barak and Nir 1987). These forms of SPD are associated with pigment dilution, though human SPD can also occur without pigment dilution (Belluci et al. 1983).

On the basis of widely varying phenotypes (Weiss et al. 1979; Lages 1987), it is likely that SPD in humans is genetically heterogeneous as it is in mice (Swank et al. 1991b, 1993). It will, therefore, be useful to have several animal models of SPD to identify the genes involved in platelet dense granule storage and secretion and eventually to develop therapies for multiple forms of human SPD.

Mice with inherited pigment dilutions are a rich source of mutations causing platelet SPD and serve as possible animal models for human HPS and CHS. We and others have found that 13 mouse pigment mutants have inherited platelet SPD (Novak et al. 1981, 1984, 1988; Ahmed et al. 1989; Swank et al. 1991a, 1991b, 1993). One mutant, beige (*bg*), also has CHS (Brandt et al. 1981). An obvious advantage of the mouse models is their ease of genetic analysis. Other investigators have identified rat (Tschopp and Zucker 1972) HPS models, and CHS has been identified in cats (Kramer et al. 1977), cattle (Meyers et al. 1979a), mink (Meyers et al. 1979b), fox (Nes et al. 1983), and rats (Nishimura et al. 1989).

Mouse pigment mutants with SPD include pallid (*pa*), Chr 2; cocoa (*coa*), Chr 3; light ear (*le*), Chr 5; reduced pigment (*rp*), Chr 7; ruby eye-2 (*ru-2*), Chr 7; mocha (*mh*), Chr 10; beige (*bg*), Chr 13; muted (*mu*), Chr 13; sandy (*sdy*), Chr 13; pearl (*pe*), Chr 13; pale ear (*ep*), Chr 19; and ruby eye (*ru*), Chr 19. The genes causing the pigment abnormalities are recessive and are scattered throughout the genome. An interesting feature of these genes is that, in most cases, the pigment dilution is accompanied by abnormalities in structure and/or function of other subcellular organelles including platelet and kidney lysosomes and platelet dense granules. For example, the two SPD mutants analyzed in this report, pale ear (*ep*) and ruby eye (*ru*), have abnormal secretion of lysosomal enzymes from kidney proximal tubule cells (Novak and Swank 1979) and, in the case of pale ear, from platelets (Novak et al. 1984). Pale ear mice also have reduced secretion of lysosomal enzymes from ammonia-treated macrophages (Brown et al. 1985). These and related facts suggest that the biosynthesis and/or processing of three separate subcellular organelles, melanosomes, lysosomes, and platelet dense granules, are related. In the case of several SPD mutants, including pale ear and ruby eye, it has been demonstrated by reciprocal bone marrow transplantation that a defect in marrow platelet progenitor cells is responsible for the SPD and that SPD can be cured by transplantation of normal marrow into mutant mice (McGarry et al. 1986). The mutations remain uncharacterized at the molecular level, although a recent report suggests that the pallid (*pa*) muta-

---

Correspondence to: R.T. Swank

Table 1. Loci mapped by RFLP analyses in interspecific backcross mice.

Gene name	Locus		Enzyme	Fragment size (kb)		Reference
	Name	Probe		bmepru/bmepru	PWK	
1. Hematopoietic insertion site 2	*His2*	His-2	*Pst*1	<u>8.1</u>	<u>5.2</u>	Askew et al. 1991
2. Terminal deoxynucleotidyltransferase	*Tdt*	TDT	*Eco*RI	<u>17.5</u>, <u>6.5</u>, <u>4.8</u>, <u>2.1</u>	<u>20.0</u>, <u>5.7</u>, <u>2.2</u>	Lo et al. 1991
3. Plasma retinol binding protein 4	*Rbp4*	pRbp-2	*Eco*RV	<u>6.4</u>	<u>3.9</u>	Chainani et al. 1991
4. Cytochrome P450 17αhydroxylase C17-20 lyase	*Cyp17*	P450$_{17\alpha}$	*Eco*RI	<u>9.4</u>, 4.8	<u>18.0</u>, 4.8	Youngblood et al. 1991
5. β1-Adrenergic receptor	*Adrb1*	β-1	*Taq*I	<u>13.0</u>	<u>9.4</u>	Frielle et al. 1987

tion is caused by an alteration in the band 4.2 gene, which encodes a cytoskeletal protein (White et al. 1992).

The recessive brachymorphic (*bm*) gene causes skeletal abnormalities including reduced overall size, reduced length of long bones, and smaller epiphyseal growth plates (Lane and Dickie 1968). It is also associated with a deficiency of the enzymes ATP sulfurylase and APS kinase (Sugahara and Schwartz 1982). These defects in turn lead to decreases in sulfated glycosaminoglycans. In addition, we have recently found (Swank, submitted) that the *bm* gene causes prolonged bleeding, though the cause is uncertain.

In this report, we identify molecular markers near the *bm*, *ep*, and *ru* hemorrhagic genes on Chr 19. A useful genetic feature of these genes is that they are relatively closely linked, lying within 10 cM. These studies lay the foundation for the eventual molecular identification of these genes by positional cloning and/or candidate gene approaches.

Materials and methods

Mice

B6C3Fe-*bm ep ru/bm ep ru* mice were purchased from The Jackson Laboratory.

PWK mice originated in Czechoslovakia and were obtained from Dr. J. Forejt (Forejt and Gregorova 1992). They have subsequently been maintained as an inbred strain (23 generations of brother × sister mating) by Verne Chapman of Roswell Park Cancer Institute. PWK mice are of the *Mus musculus musculus* species and therefore have a high probability for informative polymorphisms when compared with common laboratory strains.

B6C3Fe-*bm ep ru/bm ep ru* females were mated to PWK males. Subsequently, the backcross + + +/*bm ep ru* females × *bm ep ru/bm ep ru* males was used to produce 457 progeny. At 6–10 weeks, progeny backcross mice were phenotyped for the brachymorphic, pale ear, and ruby eye genes and sacrificed. Kidneys, livers, spleens, and brains were removed and frozen.

DNA preparation

DNA was isolated according to the method of Mann and coworkers (1986). Modifications were as follows: DNA precipitates were removed from the ethanol wash and partially air dried for 2 min to remove excess ethanol. They were then redissolved in 1 ml TE (1.0 mM Tris-HCl, 1.0 mM EDTA) buffer, quantitated by optical density measurements at 260 nm, and stored at −70°C.

Probes

cDNA probes that were known to map in the vicinity of the three genes and/or were potential candidate genes are listed (Table 1). Plasmid DNA

was isolated as described in Sambrook and colleagues (1989), and inserts were randomly labeled by random priming with alpha ^{32}P dCTP or dATP by use of the Prime-It II random primer labeling kit (Stratagene, La Jolla, Calif.).

Southern blots

A panel of common restriction enzymes was used to identify the enzyme(s) which produced informative restriction fragment length polymorphisms (RFLPs) for each probe (Table 1). Five μg of DNA was digested, and DNA fragments were separated and blotted (Southern 1975) as described in Elliott and Berger (1983). Hybridization conditions for *Adrb1* were as described by Oakey and associates (1991). Hybridization conditions for *Rbp4*, *His2*, *Cyp17*, and *Tdt* were as described in Church and Gilbert (1984).

Polymerase chain reaction (PCR)

Primer sets for analysis of microsatellites that were likely to be closely linked to the genes of interest were purchased from Research Genetics (Huntsville, Ala.). They included: *D19Mit1*, *D19Mit3*, *D19Mit4*, *D19Mit5*, *D19Mit7*, *D19Mit8*, *D19Mit9*, *D19Mit10*, *D19Mit11*, *D19Mit17*, *D19Mit24*, *D19Mit27*, *D19Mit30*, and *D19Mit38*. *D19Umi1* is a polymorphic (CA)$_n$ repeat that was identified in the region adjacent to the transgene insertion in line Tg8052 with defective kidney development (Meisler 1992; Keller et al. manuscript in preparation). *D19Umi1* was amplified with the primers 5′ AAA GGC TTT TAA TGT ATG TGT GTC A3′ and 5′ ACC AGG GCA GGT GAG TTG3′, which were obtained from the University of Michigan Oligonucleotide Synthesis Facility. Microsatellite length variations for each marker were established with parental DNA prior to analysis of backcross progeny.

PCR reactions were performed on a PTC-100 MJ Research Inc. (Watertown, Mass.) thermocycler with the following modifications to the protocol of Dietrich and coworkers (1992). Reactions were performed in 10-μl volumes in 96-well microtiter plates in reaction buffer containing 10 mM Tris-HCl, pH 8.3, 50 mM KCl, and 1.5 mM Mg Cl$_2$ with 0.4 U Taq polymerase (Boehringer Mannheim). dNTPs were at 200 μM, and forward and reverse primers were present at 100 nM. To each well, 40 ng of genomic DNA was then added. The thermocycling protocol was as follows: initial denaturation at 94°C for 5 min, then 39 cycles at 94°C for 1.5 min, 55°C for 1.5 min, 72°C for 1.5 min, and a final elongation step (10 min at 72°C).

Microsatellites that amplified poorly under our standard procedure were amplified by a "hotstart." In the "hotstart," the microtiter plate was heated at 94°C for 10 min in the absence of Taq polymerase. The plate was then maintained at 85°C, and Taq polymerase was added to each well. Subsequent steps followed the normal procedure. Markers that amplified poorly included *D19Mit8*, *D19Mit11*, *D19Mit31*, and *D19Mit38*. In the cases of *D19Mit8*, *D19Mit11*, and *D19Mit38*, the PCR buffer was changed to 20 mM Tris-HCl, pH 8.3, 100 mM KCl, and 3.0 mM MgCl$_2$ with 0.8 U Taq polymerase.

PCR products were electrophoresed on nondenaturing 8% polyacrylamide gels in 45 mM Tris-borate, 1.0 mM EDTA, pH 8.3 at 200 v for 2 h. Each gel was stained with ethidium bromide, photographed, and scored independently by two investigators.

Linkage analysis

Linkage analyses were performed with an updated version (Map Manager v2.5) of RI Manager (Manly 1993). Map Manager v2.5 allows the infer-

ence of phenotypes of loci which lie within an interval defined by typed loci that are closely linked and nonrecombinant. Order for loci was determined by minimizing the number of double recombination events. Markers found in initial analyses to be distantly linked to *bm, ep,* and *ru* were typed in a limited number of backcross progeny (<100).

Results

Backcross analysis-visual markers

Four hundred fifty-seven progeny of the interspecific back-cross were typed at the brachymorphic, pale ear, and ruby eye loci by visual inspection. The map order obtained was *bm–ep–ru,* and distances were 7.9 cM between *bm* and *ep* and 1.3 cM between *ep* and *ru.* No double crossovers were observed.

Molecular markers near the bm, ep, *and* ru genes

The complete summary of the backcross and the resulting map are presented in Table 2 and Fig. 1. The gene order, map distance between adjacent genes, total number of mice carrying recombinant chromosomes, total number analyzed for each pair of loci, and the 95% confidence intervals are given in Table 2.

Several molecular markers mapped within 1 cM of the *ru* gene (Table 2). No recombinants occurred between *ru* and *D19Umi1* among 457 progeny. Three microsatellites, *D19Mit17, D19Mit24,* and *D19Mit27,* were 0.22 cM proximal to the *ru* locus, while *Cyp17* was 0.22 cM distal to *ru.* The microsatellites *D19Mit9, D19Mit10, D19Mit38,* and *D19Mit8* were 1.1 cM distal to *ru.*

Other markers were located near the *ep* gene. *D19Mit11* was 0.44 cM proximal to *ep,* while *Tdt* was 0.87 cM proximal to *ep.* The nearest distal markers to *ep* were the microsatellites *D19Mit17, D19Mit24,* and *D19Mit27,* which were 1.1 cM distal.

At the *bm* locus, the microsatellite *D19Mit30* was 4.6 cM proximal while *D19Mit5* was 3.1 cM distal.

Other cDNA probes, in addition to *Cyp17* and *Tdt,* were chosen that were previously mapped in the vicinity of the three genes of interest and/or were candidate genes. *Rbp4* was 2.8 cM proximal to *ep* while *His2* was 4.6 cM proximal. *Adrb1,* while a plausible candidate gene for *ep* or *ru,* was found to be distantly linked to the SPD genes.

The map positions of the remaining molecular markers typed in this backcross are given in Fig. 1. *Adrb1, D19Mit1, D19Mit3, D19Mit4, D19Mit7, D19Mit8, D19Mit38, D19Mit10,* and *D19Mit30* were found to be relatively distantly linked to the three genes of interest and therefore were typed in fewer progeny, as indicated in Table 2.

It is notable that strains PWK and the stock strain B6C3Fe show a very high degree of polymorphism for microsatellite markers. We tested a total of 23 Mit markers (14 of which are listed in Table 2), and all were polymorphic. The mapping of the remaining nine Mit microsatellites (*D19Mit2, D19Mit12, D19Mit14, D19Mit15, D19Mit16, D19Mit28, D19Mit31, D19Mit40,* and *D19Mit41*) was not pursued since they are relatively distantly linked to the *bm, ep,* and *ru* genes.

Table 2. Statistical analysis of the segregation of markers. X is the number of recombinants between adjacent loci. N is the number of backcross mice typed. No double crossovers were observed in this analysis in the 21-cM interval between *D19Mit30* and *Adrb1.*

Marker	X	N	Map distance (cM)	95% Conf. interval
D19Mit30				
	20	431	4.64	2.7–6.6
bm				
	14	457	3.06	1.5–4.6
D19Mit5				
	1	456	0.22	0.0–0.6
His2				
	8	456	1.75	0.5–3.0
Rbp4				
	9	456	1.97	0.7–3.2
Tdt				
	9	457	0.44	0.0–1.0
D19Mit11				
	2	457	0.44	0.0–1.0
ep				
	5	457	1.09	0.1–2.0
D19Mit24				
	0	457	0.00	0.0–0.7
D19Mit27				
	0	457	0.00	0.0–0.7
D19Mit17				
	1	457	0.22	0.0–0.6
ru				
	0	457	0.00	0.0–0.7
D19Umi1				
	1	457	0.22	0.0–0.6
Cyp17				
	4	457	0.87	0.0–1.7
D19Mit9				
	0	148	0.00	0.0–2.0
D19Mit10				
	0	141	0.00	0.0–2.1
D19Mit38				
	0	140	0.00	0.0–2.1
D19Mit8				
	1	123	0.81	0.0–2.4
D19Mit4				
	0	120	0.00	0.0–2.5
D19Mit7				
	0	116	0.00	0.0–2.6
D19Mit3				
	3	115	2.61	0.0–5.5
D19Mit1				
	1	42	2.38	0.1–12.6
Adrb1				

Discussion

In this analysis, the chromosomal positions of five expressed genes and 15 microsatellite loci, spanning 21 cM, have been determined relative to that of the *bm, ep,* and *ru* hemorrhagic genes in an interspecific backcross of 457 mice.

Several microsatellites and cDNAs were found to be closely linked to the hemorrhagic gene loci and should prove useful as entry points for their physical mapping. They include *D19Umi1* (no recombinants with *ru* in 457 progeny) and *D19Mit24, D19Mit27, D19Mit17,* and *Cyp17,* which lie within 0.22 cM of *ru.* At the 95% confidence interval, *D19Umi1* lies within 0.65 cM of *ru.* Another useful feature of these markers is that they flank the *ru* gene. The *ep* and *ru* genes themselves, in fact, are quite close (1.3 cM). Molecular markers associated with the *ep* and *bm* loci are somewhat more distant. *D19Mit11* is 0.44 cM proximal to *ep* while *D19Mit17, D19Mit24,* and *D19Mit27* are 1.1 cM distal. Microsatellites *D19Mit30* and *D19Mit5* flank the *bm* locus at distances of 4.6 and 3.1 cM, respectively.

The map distances between the *bm, ep,* and *ru* genes (7.9 cM between *bm* and *ep* and 1.3 cM between *ep* and *ru*) and gene order obtained in this backcross agree well with available consensus maps [GBASE 1993 and the Chr 19 committee report (Guénet and Poirier 1993)].

There are significant differences between the map derived in these experiments and the consensus maps in re-
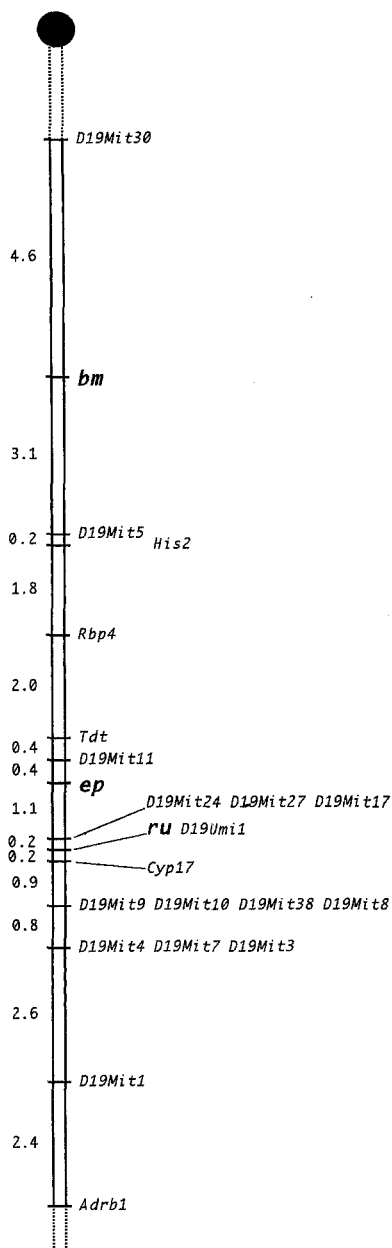
Fig. 1. A molecular genetic linkage map for mouse Chr 19 in the region of the *bm*, *ep*, and *ru* genes. Map distances between adjacent loci, determined in this backcross, are given in cM at **left.** The centromere is at figure **top.** The portions of Chr 19 between the centromere and *D19Mit30* and distal to *Adrb1* are represented by **dashed lines.**

D19Mit27 while GBASE (1993) reports *D19Mit17* in a different order, between *D19Mit4* and *D19Mit1*. Again, it is likely the former order is correct since all probes were mapped simultaneously in this cross. Also, we find *D19Mit10* is separable from *D19Mit4*, and *D19Mit1* is separable from *D19Mit7* and *D19Mit3*, while GBASE (1993) reports them as co-mapping. Finally, the orientation of microsatellite markers in relation to the centromere is in agreement with that recently reported by Eicher and associates (1993).

The fact that our mapping results are, for the most part, consistent with existing data for the known microsatellite markers used in this study strongly suggests that the brachymorphic, ruby-eye, and pale-ear mutations are not associated with gross structural rearrangements of Chr 19 sequences, but rather with minimal changes that do not significantly alter meiotic recombination frequencies.

Adrb1 was a plausible candidate gene for the SPD genes in view of the deficiency of platelet dense granule amines in the SPD mutants. Similarly, a deficiency in the *Rbp4* gene might affect pigmentation as observed in the SPD mutants. However, these studies eliminate these two genes as well as the *His2*, *Tdt*, and *Cyp17* genes as candidates for the *bm*, *ep*, and *ru* genes. No other obvious candidate genes for *bm*, *ep* and *ru* are currently present either on mouse Chr 19 or on homologous regions of the human genome.

This study provides a high resolution genetic map for the *bm–ep–ru* region of Chr 19. It provides a linkage map for positional cloning and/or the potential evaluation of candidate genes for these three genes and other genes in this region as they become available. In the case of *ru*, considerable progress toward its identification has been made in that closely linked proximal and distal flanking molecular markers have been identified. Isolation of the hemorrhagic genes may permit development of gene therapy in the mouse model. Identification of these genes will also indicate whether the many SPD genes are related at the molecular level and thus will provide insights into genes that simultaneously regulate the biosynthesis/processing of melanosomes, lysosomes, and platelet dense granules. In addition, analyses of the mechanisms of action of these genes and the eventual correction of defects in human SPD may become possible.

gard to the positions of the *bm*, *ep*, and *ru* genes relative to those of other molecular markers. This is probably owing to the fact that the consensus maps are derived from several crosses. Considering cDNA markers, a composite map lists the map order from the centromere as *Tdt–Rbp4–His2–Adrb1–Cyp17* (Guénet and Poirier 1993) while our mapping results are *His2–Rbp4–Tdt–Cyp17–Adrb1*. It is likely that the order of loci in the present map is correct since all loci were simultaneously analyzed in this backcross.

The order of microsatellite markers obtained are in most respects comparable with consensus maps. An exception is that we find *D19Mit17* maps with *D19Mit24* and

References

Ahmed, R., Lundin, L.-G., Shire, J.G.M. (1989). Lysosomal mutations increase susceptibility to anesthetics. Experientia 45, 1133–1135.

Askew, D.S., Bartholomew, C., Buchberg, A.M., Valentine, M.C., Jenkins, N.A., Copeland, N.G., Ihle, J.N. (1991). *His-1* and *His-2:* iden-

tification and chromosomal mapping of two commonly rearranged sites of viral integration in a myeloid leukemia. Oncogene 6, 2041–2047.

Barak, Y., Nir, E. (1987). Chediak-Higashi syndrome. Am. J. Pediat. Hematol. 9, 42–55.

Belluci, S., Tobelem, G., Caen, J.P. (1983). In *Progress in Hematology,* Vol. 13. E.B. Brown, ed. (New York: Grune and Stratton), p. 223.

Brandt, E.J., Swank, R.T., Novak, E.K. (1981). The murine Chediak-Higashi mutation and other murine pigmentation mutations. In *Immunologic Defects in Laboratory Animals,* M.E. Gershwin, B. Merchant, eds. (New York: Plenum Press), pp. 99–117.

Brown, J.A., Novak, E.K., Swank, R.T. (1985). Effects of ammonia on processing and secretion of precursor and mature lysosomal enzyme from macrophages of normal and pale ear mice: evidence for two distinct pathways. J. Cell Biol. 100, 1894–1904.

Chainani, M., Sampsell, B., Elliott, R.W. (1991). Localization of the gene for plasma retinol binding protein to the distal half of mouse chromosome 19. Genomics 9, 376–379.

Church, G.M., Gilbert, W. (1984). Genomic sequencing. Proc. Natl. Acad. Sci. USA 81, 1991–1995.

Depinho, R.A., Kaplan, K.L. (1985). The Hermansky-Pudlak syndrome, report of three cases and review of pathophysiology and management considerations. Medicine 64, 192–202.

Dietrich, W., Katz, H., Lincoln, S.E., Shin, H.-S., Friedman, J., Dracopoli, N.C., Lander, E.S. (1992). A genetic map of the mouse suitable for typing intraspecific crosses. Genetics 131, 423–447.

Eicher, E.M., Shown, E.P., Bhat, D., Seldin, M.F. (1993). Corrected centromere orientation for mouse chromosome 19 MIT markers. Mamm. Genome 4, 223–225.

Elliott, R.W., Berger, F.G. (1983). DNA sequence polymorphism in an androgen-regulated gene is associated with alteration in the encoded RNAs. Proc. Natl. Acad. Sci. USA 80, 501–504.

Forejt, J., Gregorova, S. (1992). Genetic analysis of genomic imprinting: an imprintor-1 gene controls inactivation of the paternal copy of the mouse Tme locus. Cell 70, 443–450.

Frielle, T., Collins, S., Daniel, K.W., Caron, M.G., Lefkowitz, R.J., Kobilka, B.K. (1987). Cloning of the cDNA for the human β-adrenergic receptor. Proc. Natl. Acad. Sci. USA 84, 7920–7924.

GBASE (1993). The genomic database of the mouse maintained at The Jackson Laboratory by D.P. Doolittle, A.J. Hillyard, L.J. Maltais, J.N. Guidi, M.T. Davisson, T.H. Roderick.

Guénet, J.-L., Poirier, C. (1993). Mouse Chromosome 19. Mamm. Genome 4(Suppl.)2, S261–S268.

Israels, S.J., McNicol, A., Robertson, C., Gerrard, J.M. (1990). Platelet storage pool deficiency: diagnosis in patients with prolonged bleeding times and normal platelet aggregation. Br. J. Haematol. 75, 118–121.

Kramer, J.W., Davis, W.C., Prieur, D.J. (1977). The Chediak-Higashi syndrome of cats. Lab. Invest. 36, 554–562.

Lages, B. (1987). Studies on storage mechanisms in the dense granules: storage pool deficient platelets. In *Platelet Responses and Metabolism,* H. Holmsen, ed. (Boca Raton: CRC Press), Vol. II, pp. 135–151.

Lane, P.W., Dickie, M.M. (1968). Three recessive mutations producing disproportionate dwarfing in mice: achondroplasia, brachymorphic, and stubby. J. Hered. 59, 300–308.

Lo, K., Landau, N.R., Smale, S.G. (1991). LyF-1, a transcriptional regulator that interacts with a novel class of promoters for lymphocyte-specific genes. Mol. Cell. Biol. 11, 5229–5243.

Manly, K.F. (1993). A Macintosh program for storage and analysis of experimental genetic mapping data. Mamm. Genome 4, 303–313.

Mann, E.A., Silver, L.M., Elliott, R.W. (1986). Genetic analysis of a mouse *T* complex locus that is homologous to a kidney cDNA clone. Genetics 114, 993–1006.

McGarry, M.P., Novak, E.K., Swank, R.T. (1986). Progenitor cell defect correctable by bone marrow transplantation in five independent mouse models of platelet storage pool deficiency. Exp. Hematol. 14, 261–265.

Meisler, M.H. (1992). Insertional mutation of 'classical' and novel genes in transgenic mice. Trends Genet. 8, 341–344.

Meyers, K.M., Holmsen, H., Seachord, C.L., Hopkins, G.E., Borchard,

R.E., Padgett, G.H. (1979a). Storage pool deficiency in platelets from Chediak-Higashi cattle. Am. J. Physiol. 237, R239–R240.

Meyers, K.M., Holmsen, H., Seachord, C.L., Hopkins, G., Gorham, J. (1979b). Characterization of platelets from normal mink and mink with the Chediak-Higashi syndrome. Am. J. Hematol. 7, 137–146.

Nes, N.B., Lium, M., Sjaastad, O. (1983). A Chediak-Higashi-like syndrome in Arctic blue foxes. Finsk-Veterinartidskr. 89, 313.

Nieuwenhuis, H.K., Akkerman, J.-W.N., Sixma, J.J. (1987). Patients with a prolonged bleeding time and normal aggregation tests may have storage pool deficiency: studies on 106 patients. Blood 70, 620–623.

Nishimura, M., Masatoshi, I., Nakano, T., Nishikawa, T., Miyamoto, M., Kobayashi, T., Kitamura, Y. (1989). Beige rat: a new animal model of Chediak-Higashi syndrome. Blood 74, 270–273.

Novak, E.K., Swank, R.T. (1979). Lysosomal dysfunctions associated with mutations at mouse pigment genes. Genetics 92, 189–204.

Novak, E.K., Hui, S.-W., Swank, R.T. (1981). The mouse pale ear mutant as a possible animal model for human platelet storage pool deficiency. Blood 57, 38–43.

Novak, E.K., Hui, S.-W., Swank, R.T. (1984). Platelet storage pool deficiency in mouse pigment mutations associated with seven distinct genetic loci. Blood 63, 536–544.

Novak, E.K., Sweet, H.O., Prochazka, M., Parentis, M., Soble, R., Reddington, M., Cairo, A., Swank, R.T. (1988). Cocoa: a new mouse model for platelet storage pool deficiency. Br. J. Haematol. 69, 371–378.

Oakey, R.J., Caron, M.G., Lefkowitz, R.J., Seldin, M.F. (1991). Genomic organization of adrenergic and serotonin receptors in the mouse: linkage mapping of sequence-related genes provides a method for examining mammalian chromosome evolution. Genomics 10, 338–344.

Sambrook, J., Fritsch, E.F., Maniatis, T. (1989). *Molecular Cloning: A Laboratory Manual,* 2nd ed. (Cold Spring Harbor, N.Y.: Cold Spring Harbor Laboratory Press).

Southern, E.M. (1975). Detection of specific sequences among DNA fragments separated by gel electrophoresis. J. Mol. Biol. 98, 503–517.

Sugahara, K., Schwartz, N.B. (1982). Defect in 3-phosphoadenosine-5′ phosphosulfate synthesis in brachymorphic mice. Arch. Biochem. Biophys. 214, 602–609.

Swank, R.T., Sweet, H.O., Davisson, M.T., Reddington, M., Novak, E.K. (1991a). Sandy: a new mouse model for platelet storage pool deficiency. Genet. Res. 58, 51–62.

Swank, R.T., Reddington, M., Howlett, O., Novak, E. (1991b). Platelet storage pool deficiency associated with inherited abnormalities of the inner ear in the mouse pigment mutants muted and mocha. Blood 78, 2036–2044.

Swank, R.T., Jiang, S.Y., Reddington, M., Conway, J., Stephenson, D., McGarry, M.P., Novak, E.K. (1993). Inherited abnormalities in platelet organelles and platelet formation and associated altered expression of low molecular weight guanosine triphosphate-binding proteins in the mouse pigment mutant gunmetal. Blood 81, 2626–2635.

Tschopp, T.P., Zucker, M.B. (1972). Hereditary defect in platelet function in rats. Blood 40, 217–226.

Weiss, H.J., Witte, L.D., Kaplan, K.L., Lages, B.A., Chernoff, A., Nossel, H.L., Goodman, D.S., Baumgartner, H.R. (1979). Heterogeneity in storage pool deficiency: studies on granule-bound substances in 18 patients including variants deficient in α-granules, platelet factor 4, β-thromboglobulin and platelet-derived growth factor. Blood 54, 1296–1319.

White, R.A., Peters, L.L., Adkison, L.R., Korsgren, C., Cohen, C.M., Lux, S.E. (1992). The murine pallid mutation is a platelet storage pool disease associated with the protein 4.2 (pallidin) gene. Nature Genet. 2, 80–83.

Witkop, C.J., Quevedo, W.C., Fitzpatrick, T.B., King, R.A. (1989). In *The Metabolic Basis of Inherited Disease,* C.R. Scriver, A.L. Beaudet, W.S. Sly, D. Valle, eds. (New York: McGraw-Hill), 6th ed., pp. 2905–2947.

Youngblood, G.L., Sartorius, B.A., Taylor, B.A., Payne, A.H. (1991). Isolation, characterization and chromosomal mapping of mouse P450 17 alpha-hydroxylase/C17-20 lyase. Genomics 10, 270–275.